ISBN: 978-3-95450-220-2 ISSN: 2673-5474 doi: 10.18429/JACoW-FEL2022-WEP05

WAKEFIELD CALCULATIONS OF THE UNDULATOR SECTION IN FEL-I AT THE SHINE

H. Liu[1], Shanghai Institute of Applied Physics, Chinese Academy of Sciences, Shanghai, China
J. W. Yan, European XFEL, Schenefeld, Germany
J. J. Guo, Zhangjiang Laboratory, Shanghai, China
T. Liu, H. X. Deng, B. Liu,
Shanghai Advanced Research Institute, Chinese Academy of Sciences,
Shanghai, China
[1]also at University of Chinese Academy of Sciences, Beijing, China

Abstract

The wakefield is an important issue in free electron laser (FEL) facilities. It could be extremely strong when the electron bunch is ultra short. Wakefileds are generated by the electron bunch and affect the electron bunch in turn which possibly destroy the FEL lasing. Wakefield study of the undulator section in FEL-I at the Shanghai high-repetition-rate XFEL and extreme light facility (SHINE) has been carried on in our work before. It shows that the wakefield has a critical impact on lasing performance. In order to diminish the impact of the wakefield, four different pipe schemes were presented. Based on sufficient calculations of resistive wall wakefields and geometry wakefields, we compare the results of these schemes and choose the optimal one for designation of the FEL-I.

INTRODUCTION

In FEL facilities the accumulative effects of wakefields always lead to critical impacts on the electron bunch, resulting in the energy spread and the deviation of transverse position. Thus the lasing performance will be decreased. The SHINE is under construction and the wakefield estimations are required. The SHINE contains three different undulator lines (FEL-I, FEL-II and FEL-III) designed for different functions. The wakefields of FEL-I undulator section have been studied in our work before [1]. However the wakefields of inner segments between undulators were calculated simply. In this paper, we calculate the wakefields of inner segments considering more exquisite structures in FEL-I. We consider gradual changed connections between beam pipes of different diameters and corrugated pipes. We compare wakefields of different schemes of inner segments. In order to estimate the roughness wakefields, we develop the original theory to make it reliable in our cases. Based on the results, we give some suggestions for the designation of the inner segments in FEL-I.

FEL-I PIPE SCHEMES

In our work before, the diameter of the vacuum chamber is 16mm and the corrugated pipes are shielded. The wakefields of the undulator section in FEL-I were studied and showed a critical impact on lasing performance. It is worth noting that the sum of geometry wakefields of the step-outs (discontinuous connections of pipes with different diameters, Figure 1) is one of the main parts of the total wakefield. Thus we consider a new scheme to diminish this part of wakefield through narrowing the aperture variation of step-outs. Since the apertures of the vacuum chambers in undulators and the gap of photon absorbers are fixed, the only changeable pipe is the vacuum chamber in the inner segment. In order to narrow the aperture variation, smaller diameter vacuum chambers should be adopted. However a smaller diameter means a lager resistive wall wakefield [2, 3] and further more, the wakefields of corrugated pipes [4–6] may be introduced because of unshielding. In addition, different materials could lead to different results.

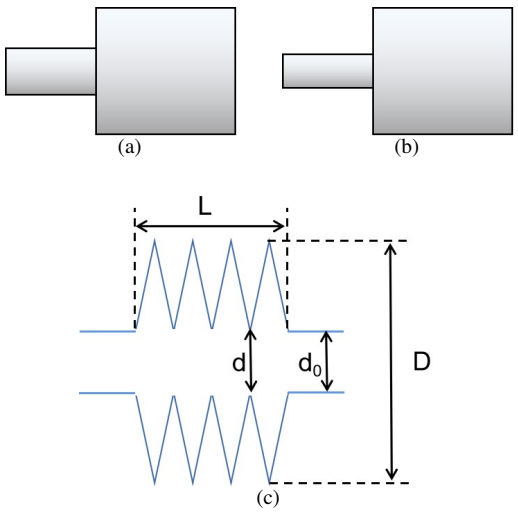

Figure 1: (a) and (b) are the diagram of two kinds of step-outs. (c) shows the geometry of the corrugated pipe.

Table 1: Parameters of Four Pipe Schemes

d_0	d	D
12	shielded	shielded
10	12	23
8	10	20
6	8	18

On the foundation that synthesize the above considerations, we proposed four different pipe schemes with three kinds of materials, copper, aluminum and stainless steel 304. The detailed parameters of the four pipe schemes are shown in Table 1. The differences of these schemes are the diame-

ISBN: 978-3-95450-220-2 ISSN: 2673-5474 doi: 10.18429/JACoW-FEL2022-WEP05

ters of pipes, d_0 is the diameter of the vacuum chambers in inner segments while the minimal diameter and the maximal diameter inside the corrugated pipe are represented by d and D as shown in Figure 1.

WAKEFIELD CALCULATION

We adopted the wakefield simulation code ECHO2D [7], which supports calculations of resistive wall wakefields and geometry wakefields respectively or in the same time. We have compared theoretical results and simulation results of the resistive wall wakefields [8] in our previous work which demonstrated great agreements. In this paper we only perform simulations. We calculate resistive wall wakefields of inner segments including vacuum chambers and photon absorbers (for scheme1 in which the corrugated pipes are shielded by copper pipes, the resistive wall wakefields of copper pipes are counted.) The results are shown in Figure 2. It is obvious that the smaller diameter scheme results in a stronger resistive wall wakefield, which is even more serious when the material is stainless steel 304.

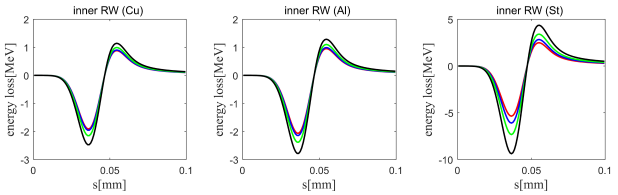

Figure 2: The sum of resistive wall wakefields of inner segments. In all the figures in this section, the results of scheme 1-4 are expressed by red lines, blue lines, green lines and black lines.

The geometry wakefields generated by two kinds of step-outs (connections from undulators and photon absorbers to the vacuum chambers of inner segments) and corrugated pipes. We calculate the geometry wakefield of every single part and the sum of them. Figure 3 shows all the results of geometry wakefields. Actually we calculate the resistive wall wakefield and the geometry wakefield of a corrugated pipe in the same time, although the resistive wall wakefield is unconspicuous. As illustrated in Figure 3, the situation is the exact opposite of the resistive wall wakefields. Reducing the aperture contributes to the decrease of the total geometry wakefields. Although the wakefield of the corrugated pipe in scheme 4 is lager than that in other schemes, geometry wakefields of step-outs constitute the main part of the sum.

In order to choose an optimal scheme, we calculate the total wakefield of the overall undulator section including the wakefields of vacuum chambers in the undulators. The results are illustrated in Figure 4. When the material of the inner segment is copper or aluminum, a smaller aperture means a smaller total wakefield. Nevertheless, when the material is stainless steel 304, the results of these four schemes turn out to be similar, because the resistive wall wakefields

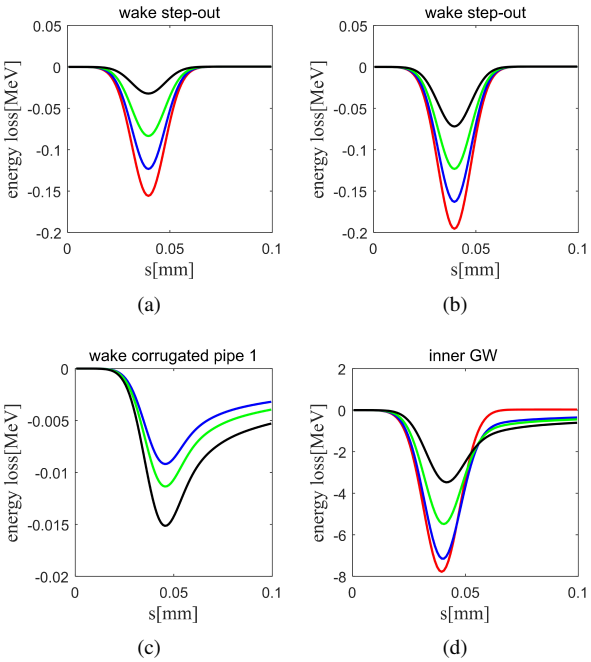

Figure 3: The geometry wakefields of inner segments. (a) and (b) show the geometry wakefields of step-outs while (c) is the result of the corrugated pipe. We calculated the sum of all the geometry wakefields and put the result in (d).

become as important as the geometry wakefileds. The wakefild of the copper inner segment is closed to the aluminum one, while the wakefield of the stainless steel inner segment is obviously too large. In addition, due to price concern we chose aluminum as the material of inner segments. Thus it is obvious that scheme 4 is the best choice. However, considering engineering issues, we chose scheme 3 as the final scheme.

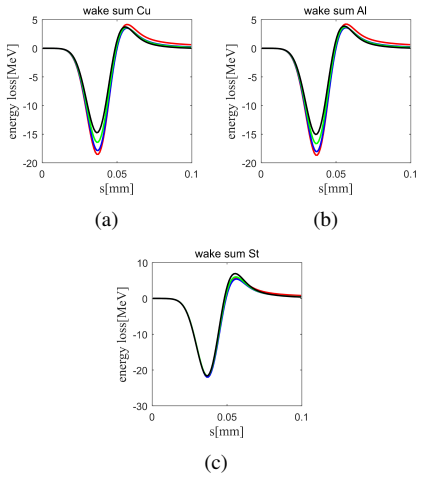

Figure 4: The total wakefield of the overall undulator section.

ISBN: 978-3-95450-220-2 ISSN: 2673-5474 doi: 10.18429/JACoW-FEL2022-WEP05

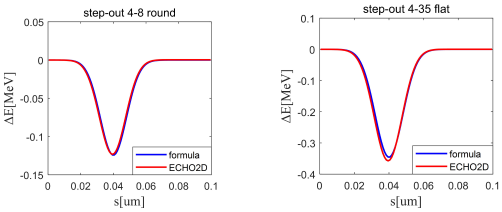

(a) (b)

Figure 5: The simulation results and theoretical results of step-out wakefileds.

DISCUSSION

In the process of finding the optimal scheme, we wondered if a taper step-out (a connection with a slope or an arc between pipes of different apertures) will be helpful in diminishing the wakefield [9]. At first we compared the simulation results with the theoretical results [10] to demonstrate the reliability. The formula we referenced is

$$Z_{||} = \frac{Z_0}{\pi} ln \frac{b}{a} \quad .$$

This formula is applied to round pipes, for flat pipes, the fraction b/a should be replaced by πb/4a.The results are shown in Figure 5. The simulation results and the theoretical results agree well. Then we calculated the wakefileds of taper step-out (both slope mode and arc mode). All the simulation results are almost the same. If we calculate not only the geometry wakefield but also add the resistive wall wakefield in the same time, the taper step-outs will generate smaller wakefields but the difference is not obvious.

In addition, we need an estimation of the roughness wakefield for the designation of FEL-I. Based on the bump mode theory proposed by K.Bane [11] (the diagram of the bump mode is shown in Figure 6), we suggested an upgrade. The original formula is

$$W_{rms} = -\alpha f \frac{cZ_0}{3^{1/4} 2^{3/2} \pi^{3/2}} \frac{r}{b\sigma_z^2} \quad ,$$

where α is a packing factor expressing the relative area on the surface occupied by the bumps.

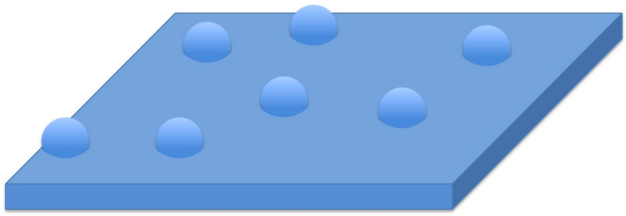

Figure 6: The diagram of the bump mode theory.

In this theory, the slant angle θ is neglected, which is an important parameter of the roughness level of surface. Moreover, the value of α is artificially selected. This leads to an overlarge value in some cases. We supposed that a bump is limited to an equal-height triangle as shown in Figure 7. We hypothesized that the wakefield generated by a bump is similar to an equal-height triangle. This hypothesis is based on our experience that the geometry wakefield mainly depends on the aperture variation. Thus the packing factor α could be expressed by the roughness slant angle θ

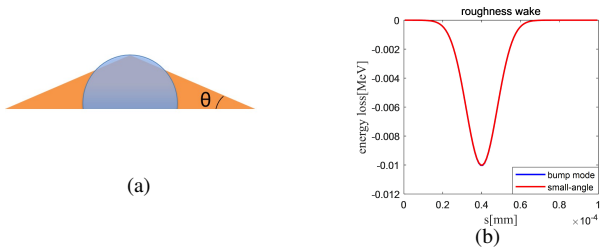

(a) (b)

Figure 7: The schematic diagram of our hypothesis and the roughness wakefields calculated based on our new theory and small-angle approximation.

$$\alpha = \frac{\pi}{4} tan^2\theta \quad .$$

The comparison of roughness wakefield calculated by our new bump mode theory and small-angle approximation [12] is shown in Figure 7. We are gratified by the great agreement, which demonstrates the reliability of our proposal.

CONCLUSION

In order to diminish the wakefields, four different pipe schemes were presented. Vacuum chambers with small diameters generate stronger resistive wall wakefields and lead to the corrugated pipes unshielded. However a smaller diameter of vacuum chamber means a smaller geometry wakefield of the step-out. The taper scheme shows little help for diminishing the wakefield. Thus the choice of optimal scheme should be based on sufficient calculations. Further more the choice of materials was also considered. The results show that the total wakefield decreases when we choose a smaller diameter. Synthetically considering engineering issues, we chose the 8mm diameter pipe scheme and aluminum as the material of vacuum chambers. We also studied the roughness wakefield in FEL-I. Based on the bump mode theory, we suggested an upgrade showing a great agreement with small-angle approximation. Thus this theory could be more reliable.

ACKNOWLEDGMENTS

The authors would like to thank Y. M. Wen and Q. S. Tang for helpful discussions. This work was partially supported by the National Key Research and Development Program of China (Grants No. 2016YFA0401901, No. 2018YFE0103100) and the National Natural Science Foundation of China (Grants No. 11935020, No. 11775293).

ISBN: 978-3-95450-220-2 ISSN: 2673-5474 doi: 10.18429/JACoW-FEL2022-WEP05

REFERENCES

[1] H. Liu *et al*., "Calculation of undulator section wakefield at the SHINE," in *Proc. SPIE, Eighth Symposium on Novel Photoelectronic Detection Technology and Applications*, vol. 12169, 2022. doi:10.1117/12.2622215

[2] K. Bane and G. Stupakov, "Using surface impedance for calculating wakefields in flat geometry," *Phys. Rev. ST Accel. Beams*, vol. 18, pp. 034401, 2015. doi:10.1103/PhysRevSTAB.18.034401

[3] B. Podobedov, "Resistive wall wakefields in the extreme anomalous skin effect regime," *Phys. Rev. ST Accel Beams*, vol. 12, iss. 4, 2009. doi:10.1103/PhysRevSTAB.12.044401

[4] K. Bane and G. Stupakov, "Impedance of a rectangular beam tube with small corrugations," *Phys. Rev. Accel. Beams*, vol. 6, p. 024401, 2003. doi:10.1103/PhysRevSTAB.6.024401

[5] K. Bane and G. Stupakov, "Corrugated Pipe as a Beam Dechirper," *Nucl. Instrum. Methods Phys. Res., Sect. A*, vol. 690, pp. 106-110, 2012. doi:10.1016/j.nima.2012.07.001

[6] I. Zagorodnov, G. Feng, and T. Limberg, "Corrugated structure insertion for extending the SASE bandwidth up to 3% at the European XFEL," *Nucl. Instrum. Methods Phys. Res., Sect. A*, vol. 837, pp. 69-79, 2016. doi:10.1016/j.nima.2016.09.001

[7] I. Zagorodnov, K. Bane, and G. Stupakov, "Calculation of wakefields in 2D rectangular structures," *Phys. Rev. ST Accel Beams,* vol. 18, p104401, 2015. doi:10.1103/PhysRevSTAB.18.104401

[8] G. Stupakov *et al*., "Resistive wall wakefields of short bunches at cryogenic temperatures," *Phys. Rev. ST Accel. Beams*, vol. 18, 2015. doi:10.1103/PhysRevSTAB.18.034402

[9] J. Arthur, *et al*., "Linac Coherent Light Source (LCLS) Conceptual Design Report," SLAC–R–593, Apr. 2002. doi:10.2172/808719

[10] M. Dohlus *et al*., "Impedances of Collimators in European XFEL," TESLA-FEL Report, Apr. 2010.

[11] K. Bane, and G.V. Stupakov, "Wake of a Rough Beam Wall Surface," in *1998 International Computational Accelerator Physics Conference*, 1998.

[12] M. Song *et al*., "Wakefield issue and its impact on X-ray photon pulse in the SXFEL test facility," *Nucl. Instrum. Methods Phys. Res., Sect. A*, vol. 822, pp.71-76, 2016. doi:10.1016/j.nima.2016.03.089